



Coupled electromechanical and electromagnetic simulation of radio frequency microelectromechanical-systems (RF-MEMS) based on compact models approach

J. Iannacci¹

Received: 2 March 2020 / Accepted: 28 May 2020 / Published online: 2 June 2020
© Springer-Verlag GmbH Germany, part of Springer Nature 2020

Abstract

In this work, a modelling approach of complete RF-MEMS (MicroElectroMechanical-Systems for radio frequency) passives is discussed. The methodology takes into account both the non-linear electromechanical and the RF behaviour, and is suitable for being implemented and automated within a standard circuit simulator. The intrinsic electromechanical core is based on a structural hierarchical model library implemented in the VerilogA programming language, compatible with most commercial EDA (Electronic Design Automation) tools and circuit development environments. A wrapping lumped element network, extracted from S-parameters measured data, accounts for the electromagnetic RF behaviour of the MEMS device. The complete non-linear network can be hierarchically instantiated within a fully functional schematic environment for mixed domain design optimisation. The model is successfully validated against static and dynamic electromechanical and RF on-wafer measurements, using an optical interferometry profilometer. In particular, this paper discusses how the mentioned approach can be extended in order to include the effects due to the presence of a wafer-level package on the RF characteristics.

1 Introduction

MEMS for RF applications (RF-MEMS) is emerging as a valuable technology solution for implementing lumped components, like variable capacitors, inductors and switches, with very high performances (e.g. high quality-factor, large tunability/reconfigurability, wide frequency operability). Because of these motivations, RF-MEMS are gaining importance as a suitable enabling technology for the synthesis of multi-standard reconfigurable platforms in wireless communication systems de Los Santos 1999; Iannacci et al. 2016a, b; Iannacci 2018).

In the design flow of RF-MEMS, simulation represents a key-step in understanding the relations existing among several parameters belonging to the electrical, mechanical and electromagnetic physical domains. Nevertheless, fast simulation tools enabling mixed-domain electromechanical and RF analysis required by RF-MEMS devices are not

readily available within integrated design environments for RF-CMOS circuit optimisation. On the other hand, employment of Finite Element Method (FEM) based software is not a viable option in the preliminary stage of the design, when dealing with several Degrees of Freedom (DoFs), due to large simulation time and computation load required. Meaningful approaches in reducing the problem complexity rely on the concept of compact modelling and have been investigated by other Authors. In particular, two among these methods are the model order reduction (Rudnyi and Korvink 2004) and the method based on equivalent electrical circuits (Senturia 2000).

In this paper, a library of compact models for elementary MEMS devices, stemming from traditional matrix-based structural mechanics and reported in Iannacci et al. (2007, 2010a, b), is exploited. Such a library includes, for instance, flexible straight beams and suspended rigid plates that, connected together, are the building blocks of a wide variety of complete RF-MEMS devices, such as switches and variable capacitors. The library is implemented in an HDL-based (Hardware Description Language) programming code, to enable simulations in the most common design environments.

✉ J. Iannacci
iannacci@fbk.eu

¹ Center for Materials and Microsystems (CMM), Fondazione Bruno Kessler (FBK), Via Sommarive, 18, 38123 Trento, Italy

The analytical mechanical models implemented in the library account both for the static and dynamic effects, i.e. elasticity and viscous damping/inertia, respectively, expressed by the following constitutive equation:

$$F = Kx + Bv + Ma \quad (1)$$

where K , B and M are the stiffness, damping and mass matrices respectively, x , v , a and F are vectors representing the position, velocity, acceleration and force/moment for all the system degrees of freedom. The four vectors contain both linear and angular DoFs. Moreover, the implemented models are completed with the inclusion of capacitance calculation and electrostatic transduction, the latter resulting in an attractive force between the suspended membranes and the actuation electrodes on the substrate when a voltage is forced across them. The developed models also account for the possible presence of release holes through the suspended plates, required by technology rules, and the fringing field effects at the edges of the structures.

In this work, the exploitation of the model library as the basis of a full non-linear mixed-domain model of complete RF-MEMS devices is investigated and discussed. In particular, the approach is demonstrated focusing on a specific device, i.e. a variable capacitor (varactor), i.e. analogue device, also operable as switched capacitor, i.e. digital device, fabricated in the RF-MEMS technology available at Fondazione Bruno Kessler (FBK), in Italy (Gaddi et al. 2005).

A surrounding equivalent lumped element network, accounting for the electromagnetic behaviour of the RF-MEMS variable/switched capacitor, is extracted from experimental data. Static and dynamic electromechanical and RF simulations of the full model are compared against experimental data, validating the adopted compact modelling approach.

In the following paragraphs the model building will be described proceeding hierarchically, i.e. starting from the intrinsic electromechanical non-linear core model, then adding lumped element networks describing RF behaviour of the intrinsic device and finally also the presence of a protective cap, as result of a Wafer-Level Packaging (WLP) encapsulation solution.

2 Electromechanical validation of the intrinsic RF-MEMS variable capacitor (varactor)

Starting from the elementary model components included in the software library, in this section the full hierarchical model used to describe the electromechanical behaviour of the complete RF-MEMS device is going to be validated. The static and dynamic behaviour (transient response) of

the RF-MEMS varactor is simulated in and compared with experimental data. Measurements are performed with a dynamic optical profilometer, based on interferometry and stroboscopic illumination.

The variable/switched capacitor is fabricated in the RF-MEMS technology available at Center for Materials and Microsystems (CMM) of Fondazione Bruno Kessler (FBK), in Italy, based on surface micromachining process of 6-inch silicon wafers (Gaddi et al. 2004). The high resistivity silicon substrate is covered by 1 μm field oxide. Polysilicon and aluminium thin-films are employed as substrate conductive layers and are used for DC actuation and RF underpass, respectively. Both substrate conductive layers are covered by silicon oxide, in order to allow metal-insulator-metal structures when the suspended layer is actuated. The suspended layer, defining MEMS structures, is made of 1.8 μm -thick electroplated gold and the air-gap is obtained by a 3 μm -thick sacrificial photoresist layer. An additional 3 μm -thick gold layer can be selectively deposited, in order to obtain stiff anchors and more rigid suspended structures.

The layout of the variable/switched capacitor studied in this paper is based on a central rigid plate in thick gold, suspended by means of four serpentine-like structures made of thin gold layer. The latter ones are preferred to simple straight beams as they reduce the elastic constant of the flexible structures, decreasing in turn the pull-in voltage, and also because they alleviate the effects of residual stress distribution within the structural gold membrane (Peroulis et al. 2003). A 3D profile of the fabricated variable capacitor is shown in Fig. 1.

The central plate has dimensions of $220 \times 220 \mu\text{m}^2$, with five $20 \times 20 \mu\text{m}^2$ squared openings distributed on the plate along each of the two in plane directions. The serpentine-like suspensions configuration and their in-plane dimensions are reported in Fig. 2.

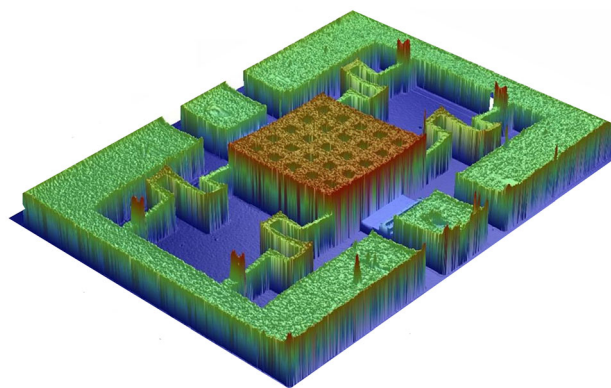


Fig. 1 3D view of the RF-MEMS variable/switched capacitor fabricated in the CMM-FBK technology. The four serpentine-like suspensions connected to the central suspended plate are visible. The colour scale represents the vertical height (Iannacci 2013)

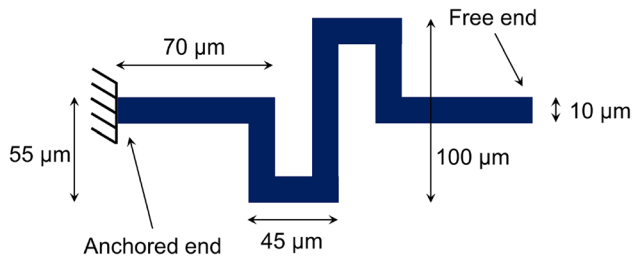


Fig. 2 Schematic of the serpentine-like suspension connected to the plate. One end is anchored while the other one is connected to the plate (Iannacci 2013)

The schematic for simulations of the hierarchical variable/switched capacitor model, implemented through the elementary components included in the MEMS software library, is shown in Fig. 3. Serpentine-like structures are realised by appropriate interconnection of straight flexible beams.

Non-idealities of the sample are taken into account by introducing a residual air gap, about 100 nm-thick, between the suspended actuated plate and the substrate, thus modelling the non-planarity of the gold membrane (see Fig. 1) due to residual stress building within gold during release. This brings to a good fitting of the simulated versus experimental pull-in/pull-out characteristic (see Fig. 4).

Subsequently, the device is simulated under transient conditions, by applying to the suspended plate a square voltage from 0 V to 4 V, with a period of 2.5 ms (400 Hz) and 50% duty-cycle. Since the variable capacitor actuation voltage is 4.9 V, the plate does not pull-into the substrate during this analysis. The simulated response compares well with experimental data, as reported in Fig. 5.

It should be noted that this type of analysis is rather critical, as it involves the full non-linear electromechanical

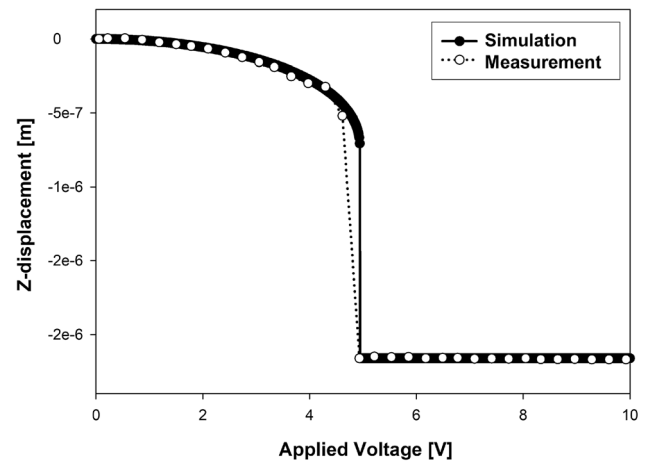


Fig. 4 Experimental versus simulated pull-in/pull-out characteristic of the variable capacitor shown in Fig. 1

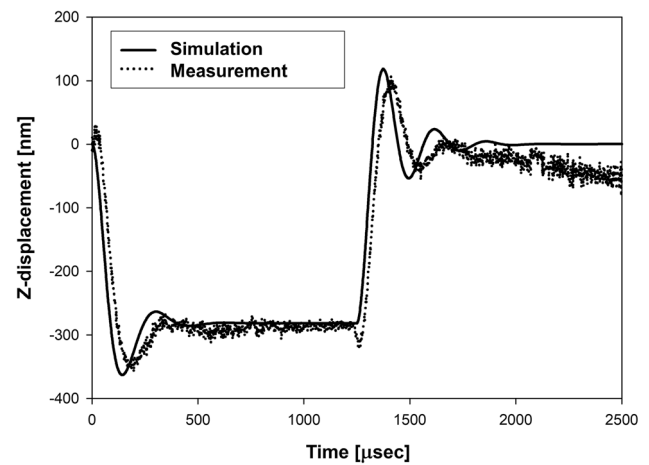
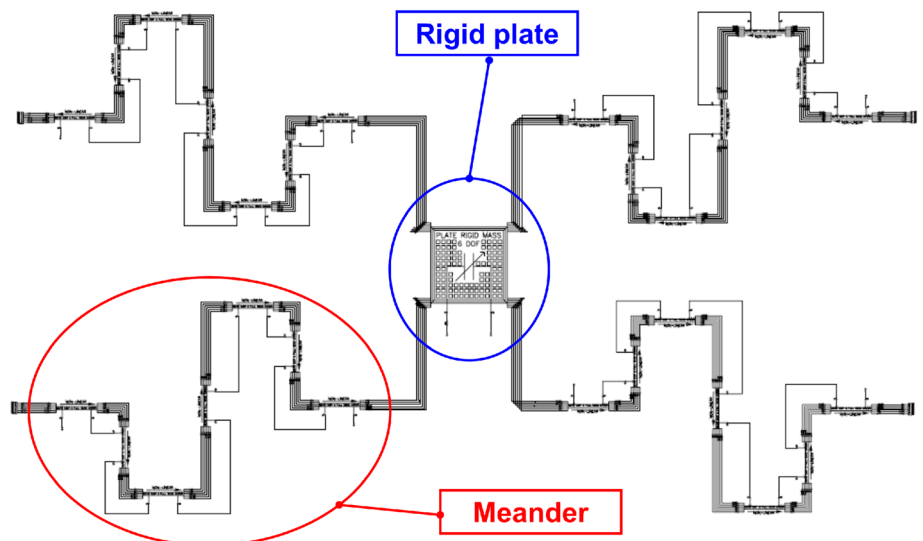


Fig. 5 Comparison between simulated and experimental transient response. The peak applied voltage is 4 V (lower than the pull-in voltage) (Iannacci 2013)

Fig. 3 Schematic of the RF-MEMS variable/switched capacitor implemented hierarchically with the compact models included in the software library



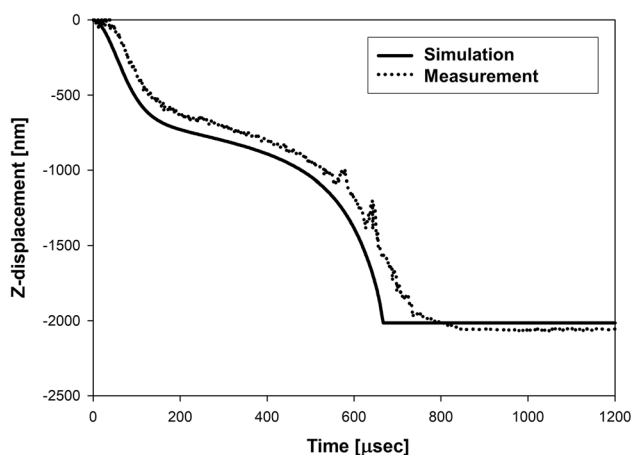


Fig. 6 Comparison between simulated and experimental transient response. The peak applied voltage is 5 V (higher than the pull-in voltage) (Iannacci 2013)

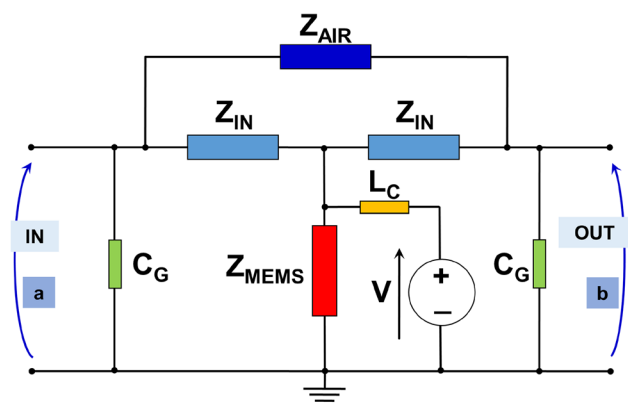


Fig. 7 Schematic accounting for all the parasitics surrounding the intrinsic RF-MEMS variable/switched capacitor. Z_{MEMS} corresponds to the schematic in Fig. 3 plus a conductance in parallel (see Table 1)

model, also including inertia and viscous damping effects, which are directly related to the observed damped oscillatory behaviour triggered at each voltage transition. The Z-displacement decrease of the experimental trace between

2 and 2.5 ms is an artefact generated by the profiling system.

The same analysis is repeated by applying a square voltage of 5 V amplitude, i.e. beyond the pull-in voltage. In this case the suspended plate collapses onto the underlying electrode, as shown in the plot in Fig. 6.

The good agreement between simulated and experimental curves is confirmed, proving that all the features determining the intrinsic electromechanical behaviour, i.e. electrostatic transduction, elastic behaviour, inertia and viscous damping, are well modelled by the compact model library.

3 Equivalent lumped element network

S-parameters (Scattering parameters) measurements of the variable capacitor are performed on-wafer through ground-signal-ground probing, at different bias voltages applied through coaxial bias-T networks. An equivalent lumped element network is wrapped around the intrinsic electromechanical device model previously validated, following an approach based on shells typical of microwave transistor modelling (Dambrine et al. 1988). Figure 7 shows the lumped element network topology.

Details and values of the lumped elements included in the network are reported in Table 1. The network accounts for the capacitive couplings, for the series inductance to ground due to the serpentine-like suspensions and for the series inductance across the input and output signal lines due to vias connecting to the underpass metal layer.

The intrinsic RF-MEMS variable capacitor (C_{MEMS} in Table 1) is modelled within the simulation environment as a sub-network corresponding to the schematic in Fig. 3, connected to a conductance in parallel that accounts for losses not included in the electrostatic transducer model. In order to apply proper controlling signal to the RF-MEMS variable/switched capacitor in the simulations, a voltage generator is connected in series with a large choke inductance (L_C), to decouple the DC voltage from the RF signal. The network parameters were extracted through circuit

Table 1 Values of the lumped components included in the schematic reported in Fig. 7

Component name	Sub-component 1	Sub-component 2	Connection
Z_{IN}	125 pH	200 mΩ	Series
Z_{AIR}	50 fF	8.48 KΩ	Parallel
Z_{MEMS}	214 fF/2.36 pF	150 μS	Parallel
C_G	25 fF	–	–
L_C	1 mH	–	–

The last column indicates if the lumped components are connected in series or in parallel. Intrinsic MEMS variable capacitance (C_{MEMS}) is implemented in the network in Fig. 7 according to the schematic reported in Fig. 3. The value of C_{MEMS} is reported for the plate in the not actuated (low capacitance) and actuated (high capacitance) state

Fig. 8 Smith chart (a) and close-up (b) of the measured and simulated S11 parameter for the variable capacitor switch, at 0, 2.8 and 5.6 V bias (Iannacci 2013)

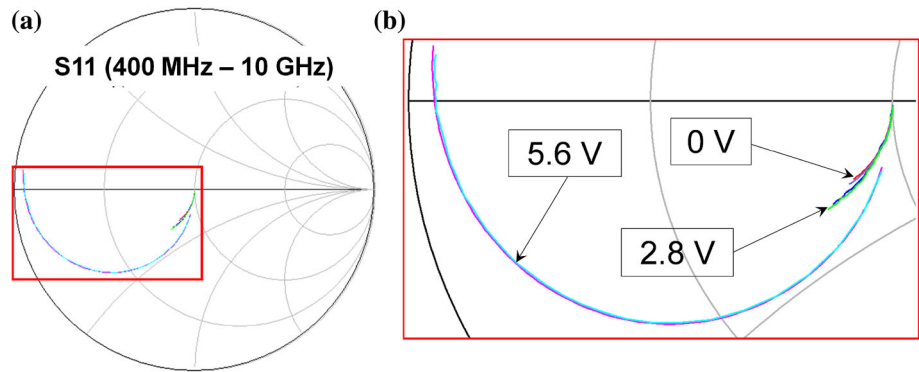
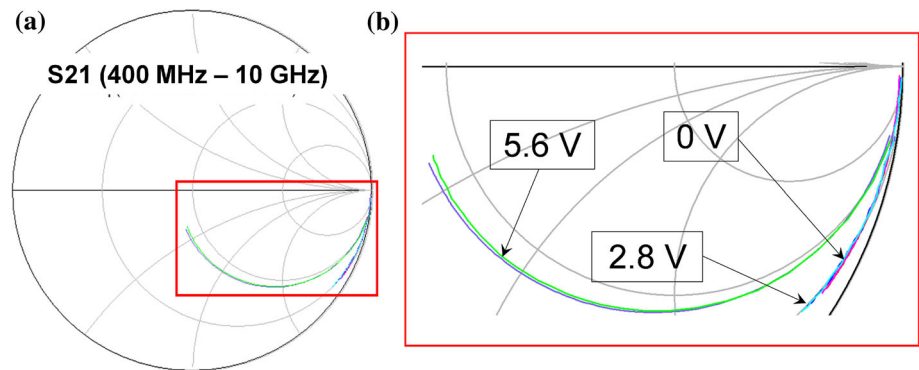


Fig. 9 Smith chart (a) and close-up (b) of the measured and simulated S21 parameter for the variable capacitor switch, at 0, 2.8 and 5.6 V bias (Iannacci 2013)



optimisation in the frequency range from 400 MHz up to 10 GHz and for all bias voltages from 0 V to 6 V. The correctness of the model topology is confirmed by obtaining constant parameter values across the whole frequency/voltage ranges, allowing only for the intrinsic non-linear electromechanical capacitance to change.

4 Validation of the complete RF-MEMS variable/switched capacitor

S-parameters simulations are shown here for a biasing voltage of 0 V, 2.8 V and 5.6 V, the last one being higher than the pull-in voltage. The simulated results are compared with the experimental ones collected for the same applied voltages. The Smith chart for the reflection parameter S11 is shown in Fig. 8.

Simulated and measured data overlap for all the three bias voltages, confirming that the compact electromechanical model combined with a fixed lumped element network can accurately predict the RF behaviour of the RF-MEMS variable/switched capacitor at different polarisation levels. The good agreement between experimental and simulated data is also confirmed by the S21 Smith chart shown in Fig. 9.

In both the Smith plots the effects of the increased shunt capacitance to ground when the plate is actuated are visible

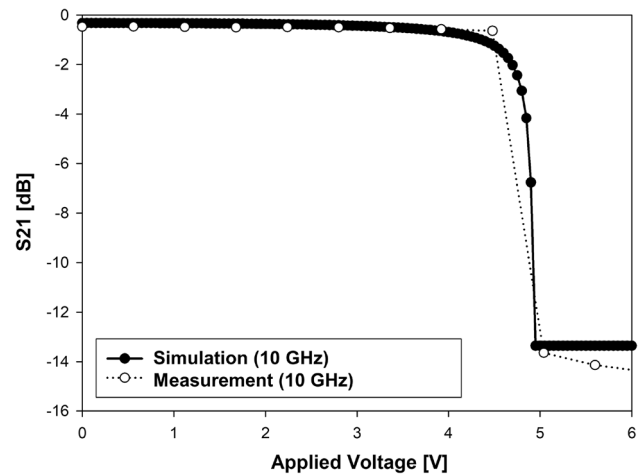


Fig. 10 Simulated versus experimental S21 parameter curves for the variable capacitor at 10 GHz with the bias voltage ranging from 0 V to 6 V, beyond the pull-in voltage (Iannacci 2013)

on the S-parameters. Concerning the reflection parameter (S11), the actuation causes a large phase rotation, which brings the impedance to the low inductive region of the chart as the frequency increases. As the MEMS capacitor is actuated, the increased isolation for the high frequency end is visible from the transmission parameter (S21), which rolls off towards the centre of the chart at higher values of the bias voltage.

Finally, the experimental versus simulated pull-in characteristic of the variable capacitor is also analysed in terms of electrical transmission coefficient. In this case, the frequency is set at 10 GHz and the S-parameters are observed for each value of the bias voltage ranging from 0 V up to 6 V. The S21 parameter plot is reported in Fig. 10, showing a good prediction of the pull-in characteristic achieved with the network of Fig. 7.

The further experimentally observed decrease of S21 between 5 V and 6 V (in the actuated state) is very likely due to the progressive flattening of the gold plate as the applied voltage is increased and, in turn, the electrostatic attraction force. This is related to residual mechanical stress within the suspended plate, as already discussed above (see Fig. 1). As the plate gets flatter, the capacitance to ground increases, leading to larger isolation. This effect is not included in the intrinsic non-linear electro mechanical model and this is reflected in the simulated S21 being perfectly flat above the pull-in voltage (between 5 V and 6 V in Fig. 10).

5 Wafer-Level Packaging (WLP) of RF-MEMS

A packaging methodology for the RF-MEMS devices discussed here was previously developed, as well (Iannacci et al. 2008; Persano et al. 2016). The technology solution is based on Wafer-Level Packaging (WLP). Redistribution of electrical signals from the MEMS wafer to the external world is provided by vertical interconnects etched in the capping silicon wafer and subsequently filled with metal, i.e. through-wafer vias (see Fig. 11).

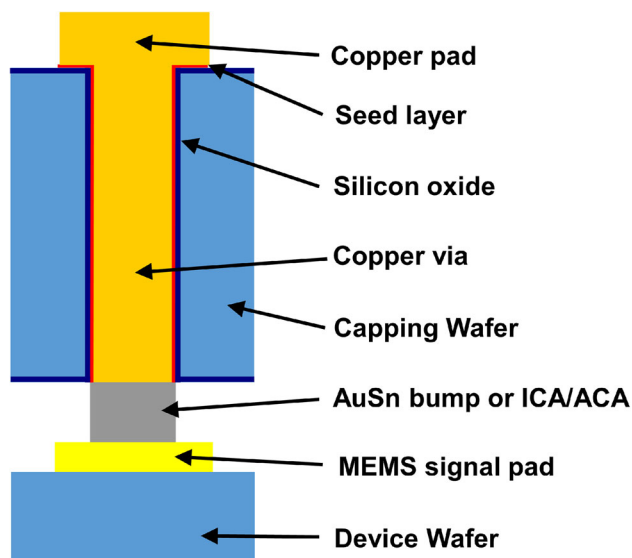


Fig. 11 Vertical section of the package. The vertical through via is in correspondence with the MEMS signal pad on the device wafer (Iannacci et al. 2006)

The silicon substrate of the capping wafer is thinned from the initial value of 525 μm down to 250–300 μm . Recesses are etched in the bottom part of the capping wafer to accommodate RF-MEMS devices, while copper top-side bumps are electrodeposited to enable on-board mounting of the encapsulated RF-MEMS chip after die singulation. The wafer-to-wafer bonding (i.e. MEMS and capping wafer) is performed by solder bumps reflow or through the use of electrically conductive adhesives (Kristiansen and Liu 1998). The proposed solution makes the integration of CMOS chips within the package also possible, leading to the fabrication of hybrid in-package RF MEMS/CMOS chips (Sosin et al. 2006).

6 Packaged RF-MEMS variable/switched capacitor model

A technology run for the package was completed and applied to reference test structures, i.e. 50 Ω Coplanar Waveguides (CPWs) and shorts (Iannacci et al. 2006). The focus here is spent around a measured CPW that is 1350 μm long, with signal and ground lines width of 116 μm and 300 μm , respectively, and gap between the lines of 65 μm . The silicon cap height is about 280 μm and its resistivity is 2 $\text{k}\Omega\text{ cm}$, while via diameter is 50 μm . Wafer to wafer bonding is performed by depositing Isotropic Conductive Adhesive (ICA) joints in correspondence with vertical vias on the bottom side of the package. S-parameter measurements collected from the described packaged CPW have been exploited to extract a lumped element network for the package plus CPW, following the same approach shown in the previous pages for the RF-MEMS variable/switched capacitor. An automated optimisation tool is also used in this case.

In the schematic network of the capped CPW, the intrinsic waveguide is modelled as an ideal CPW, with a limited air gap defined above the structure. This allows

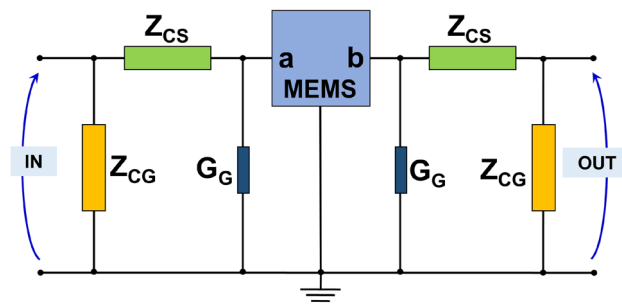


Fig. 12 Schematic of the extracted lumped elements network of the packaged variable/switched capacitor. The central part of the network is the same already reported in Fig. 7, while the additional lumped components model the package (vertical vias; ICA joints; coupling and losses through the package)

Table 2 Values of the lumped components included in the schematic in Fig. 12

Component name	Sub-component 1	Sub-component 2	Connection
Z_{CG}	80 fF	5.41 pS	Parallel
Z_{CS}	81.4 fH	850 m Ω	Series
G_G	37.9 μ F	–	–
Z_{SI}	20 fF	1.2 K Ω	Parallel

The last columns indicates if the lumped components are connected in series or in parallel. In the central block in Fig. 12 (representing the network in Fig. 7) Z_{AIR} is replaced with Z_{SI} to account for the direct coupling through the silicon cap

accounting for the vicinity of the cap to the packaged devices. After obtaining the lumped element network of the parasitic components of the capped CPW, the waveguide itself is replaced with the RF-MEMS variable capacitor network previously shown in Fig. 7. This is done under the assumption that the electromagnetic influence of the cap on the CPW is very similar to the one on the RF-MEMS variable/switched capacitor. The complete network of the variable capacitor, also accounting for the package, is reported in Fig. 12.

Details and values of the lumped elements included in the network are reported in Table 2. The central block in the schematic represents the network in Fig. 7, where Z_{AIR} is replaced with Z_{SI} . This accounts for the direct input/output coupling, which is through the silicon cap and not in air. The package is modelled as a shunt to ground parallel of a capacitance and a conductance, due to the signal to ground coupling of vias and the losses in the substrate around vertical interconnects. Moving towards the capped device, there are a resistance and an inductance in series, which model the ICA package to device wafer joints. The network is then completed by a conductance to ground in input and output, which account for the losses through the package. A resistance in parallel with a capacitance (Z_{SI}) model the direct input/output coupling through the cap.

Smith chart plots for the S-parameters of the networks in Figs. 7 and 12 are shown in Figs. 13 and 14 for the non-

actuated and actuated states, respectively. The influence of the package, related with the losses and the longer electrical length (top-side plus vertical vias), is clearly visible, especially in terms of insertion loss at 0 V bias, as expected. Isolation is relatively unaffected by parasitic effects introduced by the package.

7 Brief discussion about other exploitations of the modelling approach

The coupled-field modelling and simulation approach discussed up to here was focused on the behavioural characteristics of in-package RF-MEMS. Despite this specific addressed problem, the methodology, as well as some portions of it, can be useful in the study of a rather broad variety of problems related to diverse MEMS-based devices, as well as miniaturised (non-MEMS) components. To this regard, it can be useful splitting the discussion for what concerns the modelling of the electromagnetic (RF) and of the electromechanical characteristics.

Focusing on the RF characteristics, the modelling and simulation approach is well-suited for basically all the types of MEMS reconfigurable passives, like series or shunt ohmic or capacitive switches (i.e. switched capacitors), as well as analogue tunable capacitors (varactors) and inductors. Moreover, the equivalent network architecture

Fig. 13 Smith chart for S11 (a) and S21 (b) of the uncapped RF-MEMS variable/switched capacitor network in Fig. 7 compared with the network in Fig. 12 accounting for the the package, in the non-actuated state

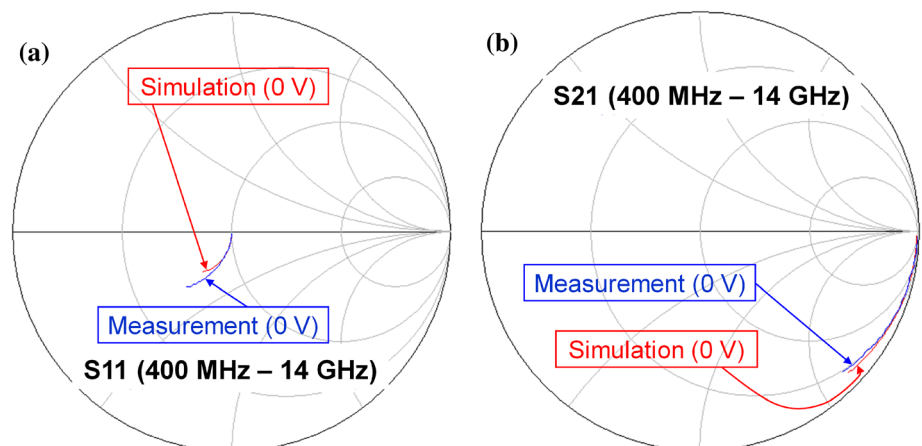
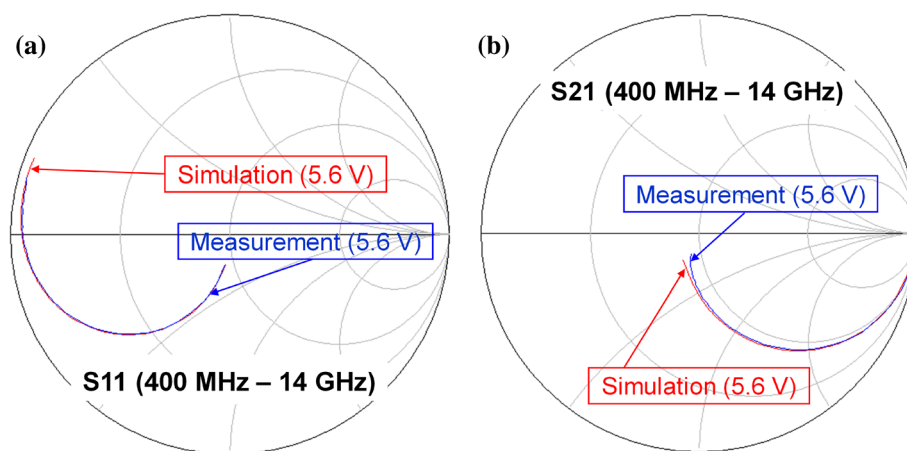


Fig. 14 Smith chart for S11 (a) and S21 (b) of the uncapped RF-MEMS variable/switched capacitor network in Fig. 7 compared with the network in Fig. 12 accounting for the the package, in the actuated state



based on lumped components is a rather powerful methodological tool for the behavioural description of RF and microwave structures. For the scope of this work, it was exploited for the electromagnetic modelling of the protective packaged applied to RF-MEMS. However, it can be easily and flexibly adapted to the description of other RF components, like stubs, resonators, couplers or splitters, as well as to other kinds of packaging and integration solutions, like wire-bonds or flip-chip mounting approaches. In addition, it should be kept in mind that the presented method can be easily hybridised with the description of active components and electronics, if based on an analytical modelling approach, thus leading to the simulation of more complex sub-systems and systems.

Eventually, a few considerations have to be developed for what concerns the electromechanical modelling approach reported in this work for the prediction of the static and dynamic behaviour of an RF-MEMS switched capacitor. As the developed mathematical models comprise all the terms of the constitutive equation of mechanical systems, the same items can be utilised for the simulation and optimisation of non-RF devices based on MEMS technology, like, for instance, accelerometers, gyroscopes, or actuators, like micro-grippers, micro-valves and micro-pumps.

8 Conclusions

In this paper, an approach for implementing non-linear electromechanical and RF models, describing the behaviour of complete RF-MEMS devices within standard circuit simulators was reported and discussed. The focus was spent around an RF-MEMS variable/switched capacitor fabricated at Fondazione Bruno Kessler (FBK), in Italy. The electromechanical behaviour of the intrinsic variable capacitor relies on the compact models available within a

MEMS software model library previously developed in an Hardware Description Language (HDL) language.

A surrounding equivalent lumped element network, accounting for the RF behaviour of the device, was extracted from S-parameters measured data. The whole network including the intrinsic variable capacitor and the extracted parasitic effects was simulated. Comparisons with experimental data show a good agreement of the S-parameters over the whole analysed frequency range (from 400 MHz to 10 GHz). Moreover, a good prediction of the variable capacitor pull-in characteristic (i.e., varying the bias voltage at a fixed frequency of 10 GHz) was achieved, showing the effectiveness of the chosen modelling approach.

Finally, the full model of a wafer-level packaged MEMS device was introduced and discussed. By exploiting experimental results of measured capped test structures (i.e. coplanar waveguides), the extraction of an equivalent lumped element network of the capped MEMS variable/switched capacitor was possible. The presented approach ultimately enables the simulation, within standard circuit design environments, of mixed RF-MEMS/CMOS in-package functional blocks for mixed-domain design optimisation.

References

- Dambrine G, Cappy A, Heliodore F, Playez E (1988) A new method for determining the FET small signal equivalent circuit. *IEEE Trans Microwave Theory Tech* 36:1151–1159. <https://doi.org/10.1109/22.3650>
- de Los Santos HJ (1999) Introduction to Microelectromechanical (MEM) microwave systems. Artech House Publishers, Boston
- Gaddi R, Bellei M, Gnudi A, Margesin B, Giacomozzi F (2004) Interdigitated low-loss Ohmic RF MEMS switches. In: Proceedings of NSTI 2004 nanotechnology conference and trade show (Nanotech 2004), pp 327–330

- Gaddi R, Gnudi A, Franchi E, Guermandi D, Tortori P, Margesin B, Giacomozzi F (2005) Reconfigurable MEMS-enabled LC-tank for multi band CMOS oscillator. In: Proceedings of IEEE MTT-S 2005 international microwave symposium (IMS2005), pp 1–4. <https://doi.org/10.1109/mwsym.2005.1516932>
- Iannacci J (2013) Practical guide to RF-MEMS. Wiley-VCH, Weinheim. <https://doi.org/10.1002/9783527680856>
- Iannacci J (2018) Internet of things (IoT); internet of everything (IoE); tactile internet; 5G—a (not so evanescent) unifying vision empowered by EH-MEMS (energy harvesting MEMS) and RF-MEMS (radio frequency MEMS). *Sens Actuators A Phys* 272:187–198. <https://doi.org/10.1016/j.sna.2018.01.038>
- Iannacci J, Tian J, Sosin S, Gaddi R, Bartek M (2006) Hybrid wafer-level packaging for RF-MEMS applications. In: Proceedings of international wafer-level packaging conference (IWLPC), pp 106–113
- Iannacci J, Gaddi R, Gnudi A. (2007) Non-linear electromechanical RF model of a MEMS varactor based on VerilogA© and lumped element parasitic network. In: Proceedings of European microwave week 2007 (EuMW), pp 544–547. <https://doi.org/10.1109/eumc.2007.4405451>
- Iannacci J, Bartek M, Tian J, Gaddi R, Gnudi A (2008) Electromagnetic optimization of an RF-MEMS wafer-level package. *Elsevier Sens Actuators A Phys* 142:434–441. <https://doi.org/10.1016/j.sna.2007.08.018>
- Iannacci J, Gaddi R, Gnudi A (2010a) Experimental validation of mixed electromechanical and electromagnetic modeling of RF-MEMS devices within a standard IC simulation environment. *IEEE J Microelectromech Syst (JMEMS)* 19:526–537. <https://doi.org/10.1109/JMEMS.2010.2048417>
- Iannacci J, Repchankova A, Faes A, Tazzoli A, Meneghesso G, Dalla Betta G-F (2010b) Enhancement of RF-MEMS switch reliability through an active anti-stiction heat-based mechanism. *Microelectron Reliab* 50:1599–1603. <https://doi.org/10.1016/j.microrel.2010.07.108>
- Iannacci J, Huhn M, Tschoban C, Pötter H (2016a) RF-MEMS technology for future mobile and high-frequency applications: reconfigurable 8-bit power attenuator tested up to 110 GHz. *IEEE Electron Device Lett (EDL)* 37:1646–1649. <https://doi.org/10.1109/LED.2016.2623328>
- Iannacci J, Huhn M, Tschoban C, Potter H (2016b) RF-MEMS technology for 5G: series and shunt attenuator modules demonstrated up to 110 GHz. *IEEE Electron Device Lett (EDL)* 37:1336–1339. <https://doi.org/10.1109/LED.2016.2604426>
- Kristiansen H, Liu J (1998) Overview of conductive adhesive interconnection technologies for LCDs. *IEEE Trans Compon Packag Manuf Technol Part A* 21:208–214. <https://doi.org/10.1109/95.705466>
- Peroulis D, Pacheco SP, Sarabandi K, Katehi LPB (2003) Electromechanical considerations in developing low-voltage RF MEMS switches. *IEEE Trans Microw Theory Tech* 51:259–270. <https://doi.org/10.1109/TMTT.2002.806514>
- Persano A, Quaranta F, Capoccia G, Proietti E, Lucibello A, Marcelli R, Bagolini A, Iannacci J, Taurino A, Siciliano P (2016) Influence of design and fabrication on RF performance of capacitive RF MEMS switches. *Microsyst Technol* 22:1741–1746. <https://doi.org/10.1007/s00542-016-2829-z>
- Rudnyi EB, Korvink JG (2004) Model order reduction of MEMS for efficient computer aided design and system simulation. In: Proceedings of 16th international symposium on mathematical theory of networks and systems, MTNS, pp 1–6
- Senturia SD (2000) *Microsystem design*. Springer, Berlin. <https://doi.org/10.1007/b117574>
- Sosin S, Tian J, Bartek M (2006) Hybrid wafer level packaging based on a capping substrate with cavities. In: Proceedings of Eurosensors XX, pp 1–4

Publisher's Note Springer Nature remains neutral with regard to jurisdictional claims in published maps and institutional affiliations.